Proceedings of the 9th International Symposium on Fluid-Structure Interactions, Flow-Sound Interactions, Flow-Induced Vibration & Noise
July 8-11, 2018, Toronto, Ontario, Canada

FIV2018-149

EVALUATION METHOD FOR IN-PLANE FEI OF TRIANGULAR ARRAY TUBE BUNDLE

Shingo Nishida
Mitsubishi Heavy Industries Ltd., Research and Innovation Center
Takasago, Hyogo, Japan

Seinosuke Azuma
Mitsubishi Heavy Industries Ltd., Research and Innovation Center
Takasago, Hyogo, Japan

Hideyuki Morita
Mitsubishi Heavy Industries Ltd., Research and Innovation Center
Takasago, Hyogo, Japan

Kazuo Hirota
Mitsubishi Heavy Industries Ltd., Research and Innovation Center
Takasago, Hyogo, Japan

Ryoichi Kawakami
Mitsubishi Heavy Industries Ltd., Nuclear Energy Systems Division
Kobe, Hyogo, Japan

Yoshihito Nishikawa
Kansai Electric Power Co., Inc.
Osaka, Osaka, Japan

ABSTRACT

Recently, tube-to-tube wear indications of triangular tube bundle steam generators caused by fluidelastic instability in the in-plane direction of U-bend region (in-plane FEI) have been reported [1].

Several experiments were conducted to investigate the characteristics of in-plane FEI by our research groups. In a series of experiments, particular characteristics of in-plane FEI were found. For example, there are the critical velocity difference between the in-plane and the out of plane directions, the difference between straight tube bundle tests and U-bend tube bundle tests etc.. To explain these characteristics, we measured unsteady fluid force acting on tubes under high temperature and high pressure steam-water flow conditions close to the steam generators. Stability analyses were conducted using the measured unsteady fluid force as inputs. Firstly, stability analyses were done to simulate straight tube bundle tests. Analysis results agreed well with experiments and it could explain the effect on critical velocity trend by number of flexible tubes and directions of vibration. Secondly, U-tube stability analyses were performed by applying unsteady fluid force coefficients for each location of U-bend tube FEM model. From the results, mechanisms of in-plane FEI were understood.

NOMENCLATURE

M_0: Mass matrix of tube bundle,
C_0: Damping matrix of tube bundle,
K_0: Stiffness matrix of tube bundle,
m_0: Mass of each tube, $k_{Xi,jY}$: Added stiffness coefficient
c_0: Damping of each tube, $c_{Xi,jY}$: Added damping coefficient
k_0: Stiffness of each tube, ρ: Fluid density
λ_n: Eigenvalue of n^{th} mode, ζ_n: Damping ratio of n^{th} mode
ω_n :Natural frequency (rad/s), ω:Frequency (rad/s)
Re: Real part, Im: Imaginary part, ρ_m: Two phase average density, f: Fluid force acting on perpendicular to flow direction
g: Fluid force acting on in-flow direction
α, σ: Fluid force coefficient of perpendicular to flow direction
τ, β: Fluid force coefficient of flow direction
i,j: Tube number, R: Tube radius, H: Transfer function
j_g: Superficial gas velocity, j_l: Superficial liquid velocity

1 INTRODUCTION

A lot of fluid force model types have been proposed to predict fluidelastic instability of tube bundle [2][3][4]. Price developed quasi-steady model and Lever developed flow retardation model. Sawadogo improved these models and this method is suitable for time historical calculation [5]. However, from a viewpoint of evaluation of periodic phenomena, unsteady fluid force model (Tanaka & Takahara model [6]) is more accurate method because the fluid force is defined in frequency domain. Furthermore, it is difficult for fluid force model based on single tube assumption to evaluate In-plane FEI behavior because In-plane FEI is caused by fluid force coupling between adjacent tubes. Phase relationship between adjacent tubes can be defined by using unsteady fluid force modeling.

Generally, unsteady fluid force measurements under two phase flow condition are very hard. However, our research group improved experimental equipment and succeed to measure fluid force coefficients under high temperature, high pressure steam-water two phase flow condition. Stability calculations were conducted by eigenvalue analyses using the measured fluid force coefficients. And calculation results showed good

agreement with the experimental results. Some parts of mechanisms of In-plane FEI were clarified by this study.

2 SOME QUESTIONS ON IP-FEI EXPERIMENT

In our recent experiments, critical velocity measurement tests have been conducted under various support conditions (natural frequency, flexible support direction, number of flexible tube), reduced velocity condition, types of test tube (straight short span or U-bend tube) and two phase flow regime[7].

Some significant characteristics were found in this test. Summary of test result is shown in Figure 2.1. (1) Difference between a single flexible tube and group of flexible tubes; Critical velocity was slightly different and instability characteristics were absolutely different. While the single flexible tube shows unclear amplitude increase above its critical velocity, group of flexible tubes show clear and sudden amplitude increase in straight short span test. (2) Difference between out-of-plane flexible test and in-plane flexible test; Non-dimensional critical velocities of in-plane flexible tube were divided into two groups (higher and lower critical velocities) by its natural frequency difference whereas that of out-of-plane flexible tube converged similar value. Basically, the critical velocities of in-plane flexible tubes were higher than that of out-of-plane flexible tubes.

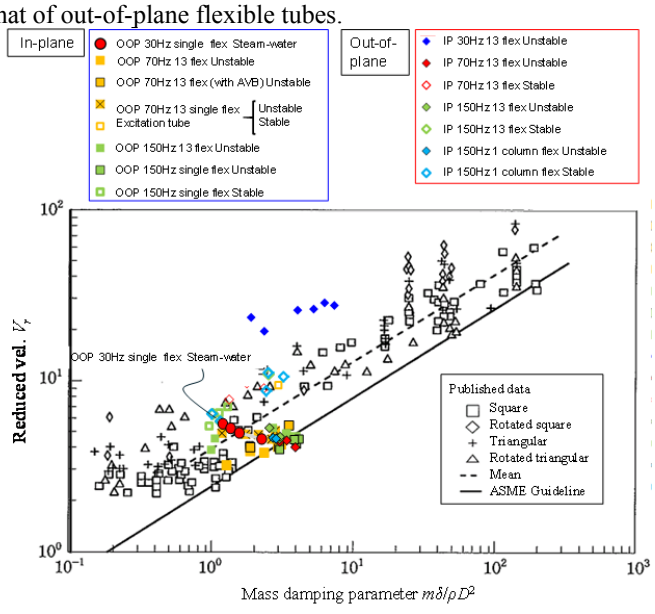

(a) Comparison between IP and OOP test (straight short span)

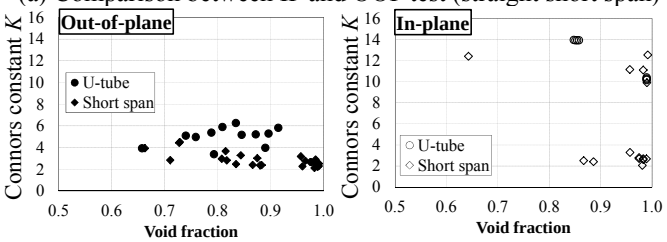

(b) Comparison between straight short span and U-tube

FIGURE 2.1: Summary of critical velocity measurement test result. [7]

However, lower critical velocity group of in-plane flexible tubes shows that the critical velocities in the in-plane direction are almost the same as out-of-plane flexible tubes.

(3) Difference between the straight short span test and the U-bend tube test; the critical velocities of the U-bend tube bundle were higher than that of straight short span tube. In addition, Difference between the straight short span and the U-bend tubes in the in-plane direction was greater than that in the out-of-plane direction.

These characteristics were investigated in this paper by stability analyses using newly measured fluid force coefficients.

3 UNSTEADY FLUID FORCE MODELING

Equation of motion of tube bundle subjected to fluidelastic instability force is written in equations below.

$$M\ddot{\mathbf{x}}+[C_0+C]\dot{\mathbf{x}}+[K_0+K]\mathbf{x}=\mathbf{0}$$

$$M_0=diag(m_0)$$

$$C_0=diag(c_0)$$

$$K_0=diag(k_0)$$

$$\mathbf{x}=\{x_1 \ \cdots \ x_i \ | \ y_1 \ \cdots \ y_i\}^T$$

$$K=\left[\begin{array}{ccc|ccc} k_{X0,0X} & \cdots & k_{X0,iX} & k_{X0,0Y} & \cdots & k_{X0,iY} \\ \vdots & \ddots & & \vdots & \ddots & \vdots \\ k_{Xi,0X} & \cdots & k_{Xi,iX} & k_{Xi,0Y} & \cdots & k_{Xi,iY} \\ \hline k_{Y0,0X} & \cdots & k_{Y0,iX} & k_{Y0,0Y} & \cdots & k_{Y0,iY} \\ \vdots & \ddots & \vdots & \vdots & \ddots & \vdots \\ k_{Yi,0X} & \cdots & k_{Yi,iX} & k_{Yi,0Y} & \cdots & k_{Yi,iY} \end{array}\right] \quad C=\left[\begin{array}{ccc|ccc} c_{X0,0X} & \cdots & c_{X0,iX} & c_{X0,0Y} & \cdots & c_{X0,iY} \\ \vdots & \ddots & & \vdots & \ddots & \vdots \\ c_{Xi,0X} & \cdots & c_{Xi,iX} & c_{Xi,0Y} & \cdots & c_{Xi,iY} \\ \hline c_{Y0,0X} & \cdots & c_{Y0,iX} & c_{Y0,0Y} & \cdots & c_{Y0,iY} \\ \vdots & \ddots & \vdots & \vdots & \ddots & \vdots \\ c_{Yi,0X} & \cdots & c_{Yi,iX} & c_{Yi,0Y} & \cdots & c_{Yi,iY} \end{array}\right] \tag{3.1}$$

S.S. Chen defined unsteady fluid force as next form [8].

$$f_i=-\rho\pi R^2\sum_{j=1}^{n}\left(\alpha_{ij}\frac{\partial^2 u_j}{\partial t^2}+\sigma_{ij}\frac{\partial^2 v_j}{\partial t^2}\right)-\rho RU\sum_{j=1}^{n}\left(\bar{\alpha}'_{ij}\frac{\partial u_j}{\partial t}+\bar{\sigma}'_{ij}\frac{\partial v_j}{\partial t}\right)+\rho U^2\sum_{j=1}^{n}\left(\alpha''_{ij}u_j+\sigma''_{ij}v_j\right)$$

$$g_i=-\rho\pi R^2\sum_{j=1}^{n}\left(\tau_{ij}\frac{\partial^2 u_j}{\partial t^2}+\beta_{ij}\frac{\partial^2 v_j}{\partial t^2}\right)-\rho RU\sum_{j=1}^{n}\left(\bar{\tau}'_{ij}\frac{\partial u_j}{\partial t}+\bar{\beta}'_{ij}\frac{\partial v_j}{\partial t}\right)+\rho U^2\sum_{j=1}^{n}\left(\tau''_{ij}u_j+\beta''_{ij}v_j\right) \tag{3.2}$$

Equation (3.1) can be written in state space form as follows.

$$\left[\lambda\begin{bmatrix}K_0+K & \mathbf{0}\\ \mathbf{0} & -M\end{bmatrix}^{-1}\begin{bmatrix}C_0+C & M\\ M & \mathbf{0}\end{bmatrix}+\mathbf{I}\right]=\mathbf{0} \tag{3.3}$$

Stability analysis can be conducted by solving generalized eigenvalue problem of equation (3.3). Natural frequencies and damping ratios are expressed using solution of this eigenvalue problem as shown below.

$$\zeta_n=-\mathrm{Re}(\lambda_n)/abs(\lambda_n)$$

$$\omega_n=\mathrm{Im}(\lambda_n) \tag{3.4}$$

Unsteady fluid forces in the equation (3.2) should be measured under two phase flow condition simulated actual steam generator.

4 FLUID FORCE MEASUREMENTS

Non-dimensional unsteady fluid force coefficient in equation (3.2) is defined as a function of reduced velocity fD/U. Therefore, fluid forces must be measured in various flow velocity and excitation frequency conditions. The test conditions are shown in Table 4.1. The test equipment is shown in Figure 4.1. The fluid forces were measured by the straight short span triangular tube bundle. Measurement tubes consisted of oscillating measurement tube and adjacent stationary measurement tubes. Fluid forces acting on each measurement tubes and displacement of measurement tubes were measured.

Transfer function between tube displacement and fluid force is calculated and converted to fluid force coefficient by following equations.

$$\bar{\alpha}' = -\frac{\mathrm{Im}(H)}{\omega \rho_m R U}, \quad \alpha'' = \frac{\mathrm{Re}(H)}{\rho_m U^2} \qquad (4.1)$$

Although this kind of equipment is commonly used for unsteady fluid force measurements, this system was improved for measurement of small level fluid force. This system allowed precise force measurement under huge internal pressure.
Examples of measured fluid coefficients are shown in Figure 4.2.

TABLE 4.1: Fluid force measurement test condition

Flow vel.	2.3-5.8m/s	**Oscillation amplitude**	1mm
Volumetric gas flow rate	β=0.7-1.0	**Oscillation frequency**	5Hz-50Hz
Tube dia.	19.05mm	**Temp.**	276 deg.C
Tube length	161mm/ 110mm	**Fluid**	Steam-water two phase
P/D	1.33	**Pressure**	5.88MPa

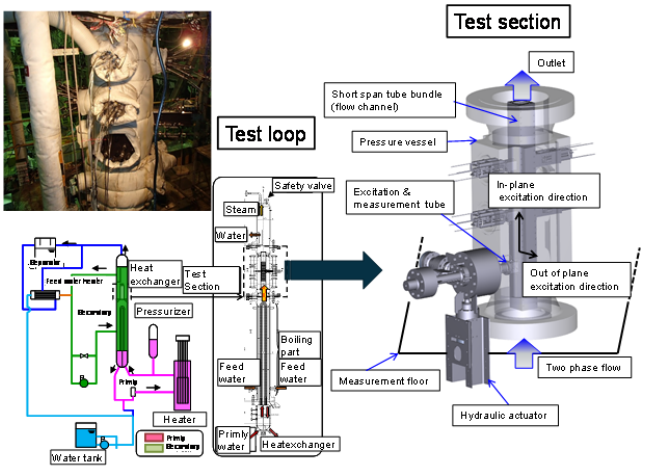

(a) Steam-water two phase test loop

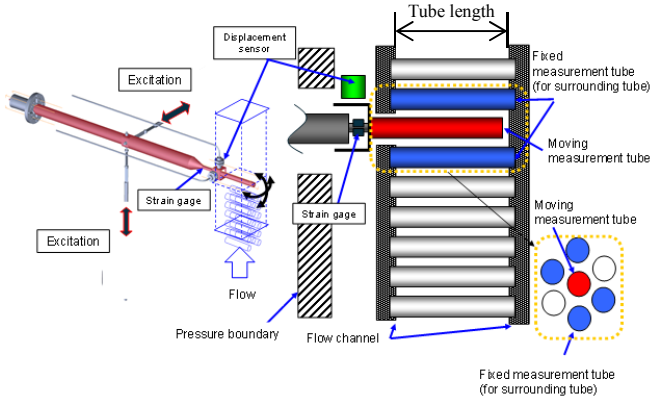

(b) Test section

FIGURE 4.1: Fluid force measurement equipment

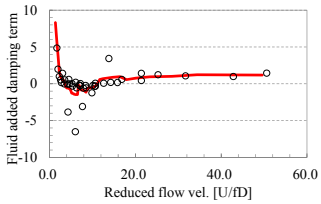

(a) OOP fluid added damping

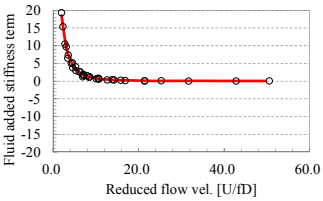

(b) OOP fluid added sttiffness

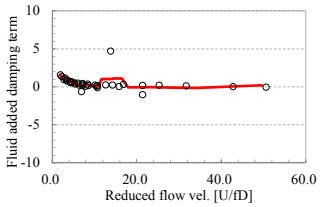

(c) IP fluid added damping

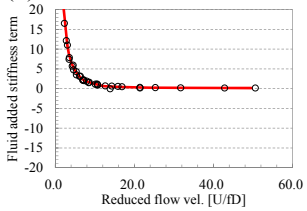

(d) IP fluid added sttiffness

FIGURE 4.2: Examples of measured fluid coefficients

5 CALCULATION RESULT AND COMPARISON

Stability analyses in the same conditions as the critical flow velocity measurement tests were conducted using measured fluid coefficients. Following assumptions were applied for the calculations. Only no influence of friction damping conditions were employed in both calculations and tests.

(1) Same (or anti-symmetric) fluid force coefficients were used for tubes located at symmetrical position to perpendicular to flow direction.
(2) Fluid forces of perpendicular to flow direction acting on tubes located at the same column with tube oscillating to flow direction is negligible.
(3) Mass damping parameter is changed by tuning void fraction (i.e. fluid density). Although mass ratio and damping ratio is thought to be independent parameter in general, damping ratio is 1% for simplicity in the calculation (assumed structural damping).
(4) Influence of natural frequency shift on fluid force coefficients is negligibly small. Strictly speaking, added stiffness and added damping by fluid force affects natural frequency of a tube and this changes frequency-dependent fluid force. In order to simulate this effect precisely, iterative calculations are needed, However, frequency shift is small except divergence mode, and divergence mode is out of scope in this calculation.
(5) Fluid coupling forces (non-diagonal term in equation 4.1) act only on adjacent tubes.

5.1 Out-of-plane flexible straight short span tube

Calculation result of single flexible tube and 13 group of flexible tubes are shown in Figure 5.1. In both conditions, lowest stability boundary agrees well with experimental result. All of experimental results in the graphs are SF_6-ethanol condition except 30Hz out-of-plane steam-water test. Both stability maps showed peninsular-like unstable region. This indicates existence of more than one instability boundary for the same mass damping parameter. In general, once tube goes unstable, tube doesn't become stable again by increasing flow

velocity in upper stable region because tube amplitude grows on a particular unstable phase relationship. As a result, lowest stability boundary tends to appear in the experiment. In comparison between single and group flexible conditions, although lowest stability boundary is almost the same reduced flow velocity, group of flexible tubes have broader unstable region. This is because non-diagonal terms of added stiffness couple instability of each tube that has slightly different characteristics. And this effect makes wider and greater unstable region. This explains experimental results; while single flexible tube shows unclear amplitude inclement at its critical velocity, group flexible tube shows clear and sudden amplitude increments.

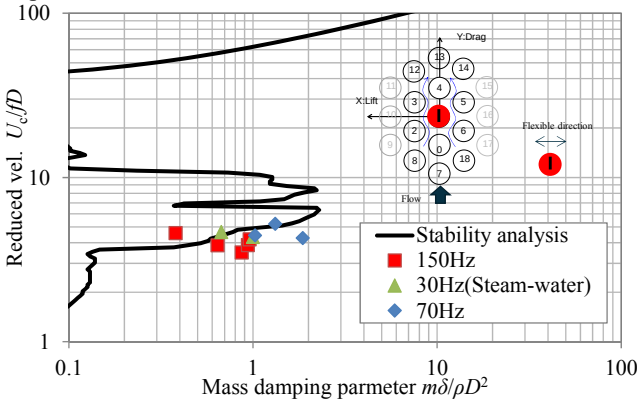

(a) Single flexible

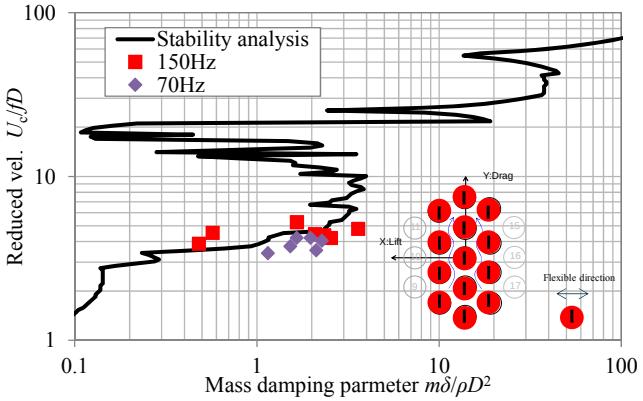

(b) 13 tubes flexible

FIGURE 5.1: Stability analysis result for out-of-plane flexible conditions

5.2 In-plane multiple flexible straight short span tube

Calculation results of 5 tubes in 1 column flexible and 13 group of flexible tubes are shown in Figure 5.2. In both conditions, calculated stability boundary characteristics show reasonable agreement with experiments. Both stability maps have narrow and complicated unstable region. This is result from that, equivalent damping ratio is vary greatly by its unstable mode shape because in-plane direction FEI is caused by stiffness coupling of each tube. Stiffness coupled unstable system could have various intensity of instability by their relative phase relationship between each tube. Regarding 13 group of flexible tubes, experimental results of 30Hz tuned tube agree well with the calculated upper stability boundary. This suggests that 30Hz tuned tubes leaped lower stability boundaries and set into unstable at upper stability boundaries. This is assumed to be caused by the following reasons; because 30Hz tuned tube is susceptible to flow drag force and random excitation, tube geometry tend to perturb and phase relationship of weak unstable mode likely to be disturbed. Comparing in-plane and out-of-plane flexible conditions, lowest critical velocity of out of plane is lower than that of in-plane flexible conditions in the low mass damping parameter region (about below 4; frequently used in actual SG).

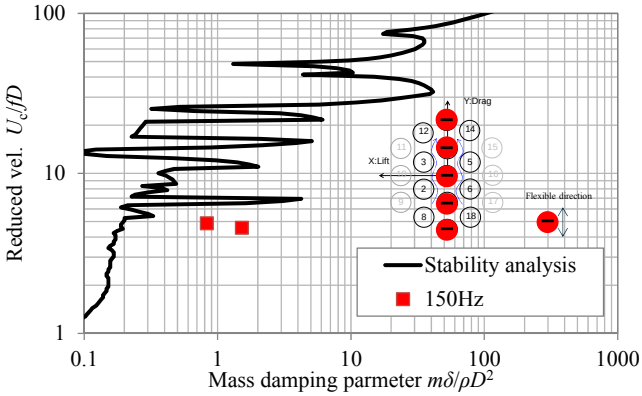

(a) 5 tubes 1 column flexible

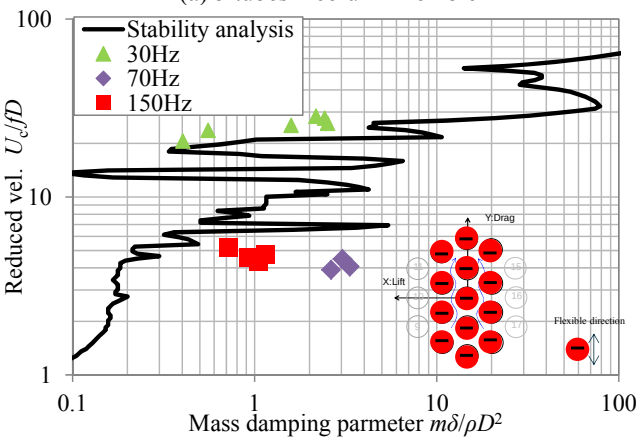

(b) 13 tubes flexible

FIGURE 5.2: Stability analysis result for in-plane flexible conditions

5.3 U-bend tube

On a series of U-bend tube tests, they were conducted under various flow distributions (flow velocity, void fraction). Because fluid added stiffness and damping vary at local U-tube position by flow distribution, various fluid force coefficients were applied at each node of U-bend tube FEM model. Schematic of analytical model is shown in Figure 5.3. The calculation results are compared with experimental results by the changing trend of natural frequency and damping ratio against flow velocity. Because detailed flow velocity distributions (estimated by bi-optical probe measurement

result) were measured only in the conditions close to critical velocity, flow velocity distribution pattern was used for calculations of all average flow velocity condition and multiplying factor was applied by the ratio of measured average flow velocity to intended condition. Measured void fraction (fluid density) distribution was used for all average flow velocity condition. Non-uniform flow condition was applied for all calculations.

Total equivalent damping of the system was evaluated by sum of calculated damping ratio (structural damping in the air is set to zero) and measured structural damping in the air.

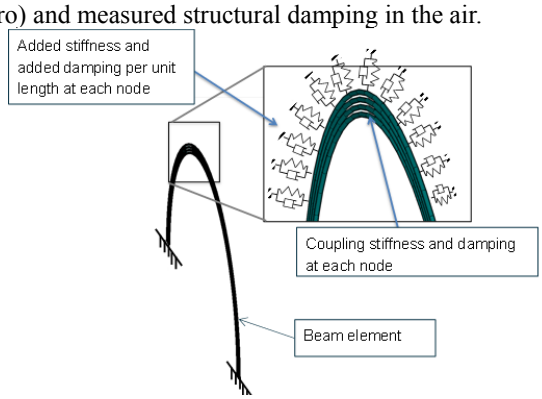

FIGURE 5.3: Schematic of analytical model for U-tube

5.3.1 Out-of-plane flexible U-bend tube (single flexible tube)

Calculation of 4 adjacent AVB free conditions was conducted. Support condition and measured flow distribution are shown in Figure 5.4. The calculation results are shown in Figure 5.5. The calculated critical velocity (turning point of damping ration to minus value) agrees well with the test result. Although calculated results of damping ratios are not completely agree with the measured results other than close to critical velocity, this is unavoidable because the actual flow velocity was not measured in other conditions. However, calculation results showed well the trend found in the experiments that damping ratio increased again after once system went unstable. This trend can be understood vertical slice of figure 5.1(a). Damping ratio could be increased again after critical velocity depending on mass damping parameter (damping ratio is measured only in stable condition by curve fitting method). In addition, calculated natural frequency agrees well with experiment in all conditions.

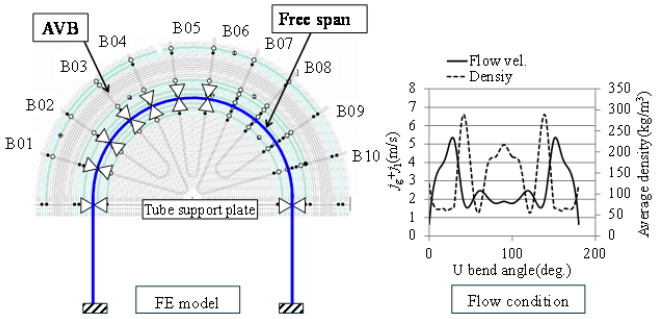

FIGURE 5.4: Measured Flow distribution and support condition (Out-of-plane flexible U-tube)

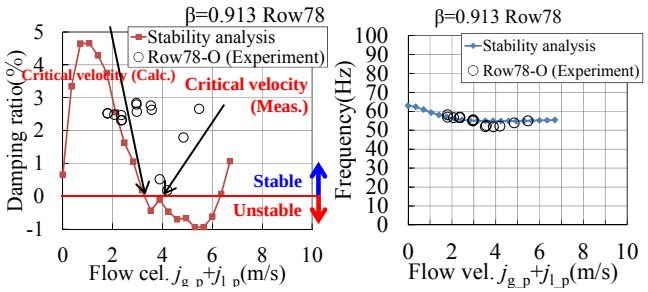

FIGURE 5.5: Calculation result of out-of-plane flexible U-tube

5.3.2 In-plane flexible U-bend tube (4tube 1 column flexible tube)

Calculations of all AVB free condition was conducted. The support condition and measured flow distribution are shown in Figure 5.6. The calculation results are shown in Figure 5.7. The calculated critical velocity agrees well with the test result. The calculated results of damping ratios are not completely consistent with the measurements other than close to critical velocity by the same reason with out-of-plane flexible calculations. Regarding the natural frequency calculation results, the difference between the measurements and calculations is large compared to the out-of-plane flexible condition. The reason of this difference is thought to be the characteristic that natural frequency shift of in-plane flexible condition is more sensitive to flow distribution because in-plane FEI is caused by stiffness coupling of group flexible tube.

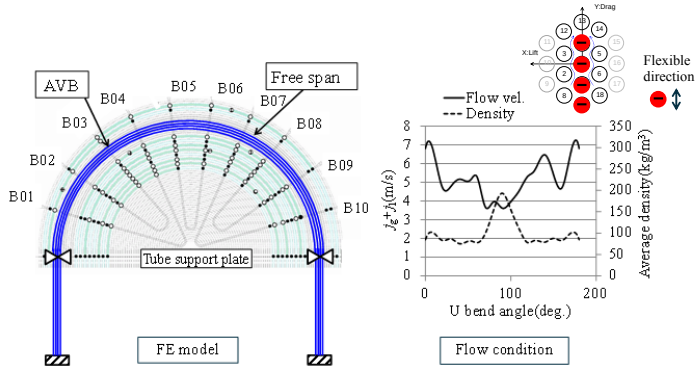

FIGURE 5.6: Measured Flow distribution and support condition (in-plane flexible U-tube)

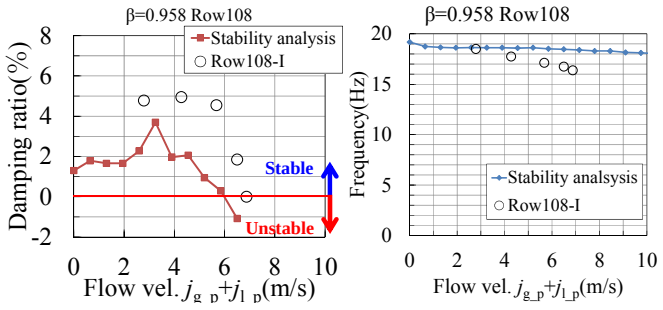

FIGURE 5.7: Calculation result of in-plane flexible U-tube

6 DISCUSSION

From comparison between the straight short span test of in-plane flexible condition and the out-of-plane flexible condition, it is found that criteria for out-of-plane flexible condition can be used conservatively. However, two groups of critical velocity in Figure 5.2(b) appeared in in-plane straight short span test and lower group is close to out-of-plane flexible condition. On the other hand, the critical velocities of in-plane flexible U-tube test converged to single group. This critical velocity was close to upper group of straight short span test. To investigate this difference, both of the distributed and the flat flow condition are applied to the calculations. The distributed conditions are the same as those used in Chap.5. The flow condition same as average value of distributed condition is applied to all position of U-tube in the flat condition. For simplicity, straight part of the tubes were removed from FEM model and 6DOF fixed at TSP position.

The calculation result is shown in Figure 5.8. Basically, flat conditions are the same as the straight short span condition. For the out-of-plane flexible condition, it is found that flow distribution shifts added damping trend curve to higher reduced velocity and this delays appearance of instability. This results from stabilizing effect of relatively slow flow velocity position. Although this effect always delays instability from flat condition, quantitative magnitude relationship compared to evaluation by effective velocity depends on flow distribution and fluid force characteristics. Same averaging effect is also found in in-plane flexible condition. In the in-plane flexible flat flow distribution condition, sharp peaks and notches are found in added damping ratio trend curve. This corresponds to sharp peninsular-like unstable areas in stability map (Figure 5.2). However, these peaks and notches disappeared in the distributed flow condition. This is caused by the trend that sharp peninsular-like unstable areas have weak negative damping characteristics and susceptible to flow distribution. This is the in-plane instability mechanisms, that is, stiffness coupling generate instability. Small unstable areas can easily be stabilized by stabilizing effect of U-tube parts that have positive damping. As a result, lower small unstable region disappears and upper region appears as first instability mode.

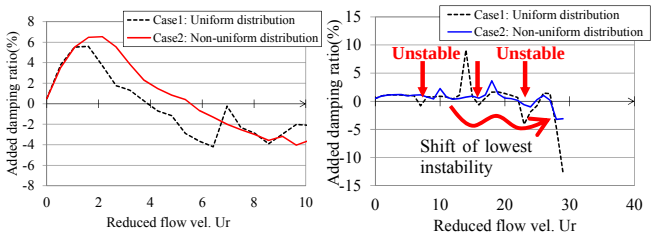

(a) Out-of-plane direction (b) In-plane direction

FIGURE 5.8: Comparison between uniform and distributed flow condition

CONCLUSION

Stability analyses were conducted using the unsteady fluid force coefficients, which were newly measured and highly accurate. The calculation results showed good agreement with the test results in various support conditions, various flow conditions and short span/U-bend tube conditions. Following conclusions were derived by comparing the measurements with the calculations.

(1) Basically, critical flow velocity of out-of-plane direction is lower than that of in-plane direction. This means criteria for out-of-plane direction can be used for all direction conservatively.

(2) Difference of critical velocity between U-bend tube and short span is caused by averaging effect of flow distribution. In particular, this averaging effect stabilize small unstable areas of in-plane flexible conditions. As a result, lower critical velocity group found in straight short span tests didn't appear in U-bend tube tests. This indicates that lower instability is not likely to occur in steam generators. However, this depends on flow distribution.

ACKNOWLEDGMENTS

This experimental work has been carried out as a Japanese government-subsidized R&D project, "The Safety Improvement of Nuclear Facilities" with the participation of The Kansai Electric Power Co., Inc., Kyushu Electric Power Co., Inc., The Japan Atomic Power, The Institute of Applied Energy, And Mitsubishi Heavy Industries, LTD.

REFERENCES

[1] Southern California Edison, 2012 "San Onofre Nuclear Generating Station Unit 2 Return to Sercice Report", *Web on NRC*, pp. 1-54

[2] Price, S. J., 1995, "A Review of Theoretical Models for Fluidelasitc Instability of Cylinder Arrays in Cross Flow". *Journal of Fluids and Structures, Vol.**9*** pp.463-518

[3] M. P. Paidoussis et al., 1987, "Flow Induced Instabilities of Cylindrical Structures", *Applied Mechanics Reviews*, **40**, pp.163-175.

[4] J. H. Lever, 1982, A Theoretical Model for Fluid-Elastic Instability in Heat Exchanger Tube Bundles, *Journal of Pressure Vessel Technology*, *Vol.* ***104***, pp. 147-158.

[5]T. Sawadogo, 2014, Fluidelastic instability study in a rotated triangular tube array subject to two-phase cross-flow. Part I: Fluid force measurements and time delay extraction, *Journal of Fluids and Structures*, *Vol.49*, pp. 1-15.

[6] H. Tanaka, S. Takahara, "1981, Fluid Elastic Vibration of Tube Wrray in Cross Flow". *Journal of Sound and Vibration*, *Vol.* ***77(1)***, pp. 19-37.

[7]S. Azuma et al., "Investigation of Critical Flow Velocity of a Triangular U-tube Bundle Subjected to Two-phase Flow" *Proceedings of the 9th International Symposium on Fluid-Structure Interactions, Flow-Sound Interactions, Flow-Induced Vibration & Noise*

[8] S.S. Chen, 1983. "Instability Mechanisms and Stability Criteria of a Group of Circular Cylinders Subjected to Cross-Flow.Part1 : Theory". *Transaction of ASME, Vol.**105**,* pp. 52-58.